ACS OMEGA

http://pubs.acs.org/journal/acsodf

Article

pH-Responsive Nano-transferosomes of Purpurin-18 Sodium Salt and Doxorubicin for Enhanced Anticancer Efficiency by Photodynamic and Chemo Combination Therapy

Sooho Yeo,* Min Je Kim, Il Yoon,* and Woo Kyoung Lee*

Cite This: *ACS Omega* 2023, 8, 16479−16490

Read Online

ACCESS | Metrics & More | Article Recommendations

ABSTRACT: Cancer is a devastating disease and a major human health concern. Various combination treatments have been developed to combat cancer. To obtain superior cancer therapy, the objective of this study was to synthesize purpurin-18 sodium salt (P18Na) and design P18Na- and doxorubicin hydrochloride (DOX)-loaded nano-transferosomes as a combination of photodynamic therapy (PDT) and chemotherapy for cancer. The characteristics of P18Na- and DOX-loaded nano-transferosomes were assessed, and the pharmacological efficacy of P18Na and DOX was determined using the HeLa and A549 cell lines. The nanodrug delivery system characteristics of the product were found to range from 98.38 to 217.50 nm and −23.63 to −41.10 mV, respectively. Further, the release of P18Na and DOX from nano-transferosomes exhibited a sustained pH-responsive behavior and burst in physiological and acidic environments, respectively. Accordingly, the nano-transferosomes effectively delivered P18Na and DOX into cancer cells, with less leakage in the body, and exhibited pH-responsive release in cancer cells. A photo-cytotoxicity study to HeLa and A549 cell lines revealed a size-dependent anti-cancer effect. These results suggest that the combined nano-transferosomes of P18Na and DOX are effective in the combination of PDT and chemotherapy for cancer.

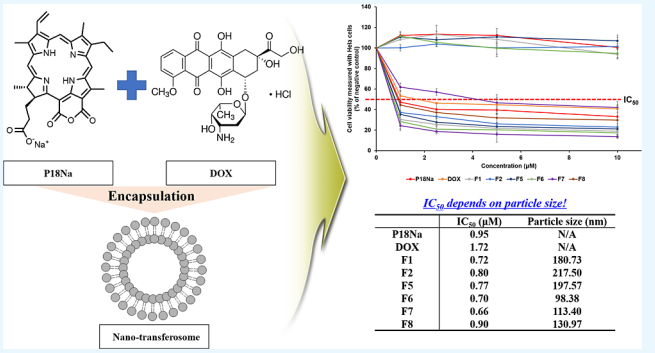

	IC_{50} (μM)	Particle size (nm)
P18Na	0.95	N/A
DOX	1.72	N/A
F1	0.72	180.73
F2	0.80	217.50
F5	0.77	197.57
F6	0.70	98.38
F7	0.66	113.40
F8	0.90	130.97

INTRODUCTION

Many diseases and activities, such as gene mutations, protein misfolding, and cell malfunction, are attributed to abnormal biological processes at the molecular level.[1] Cancer is a destructive disorder caused by the unstoppable cell growth, which is triggered by a series of genome mutations and their subsequent propagation throughout the body.[2−4] Currently, conventional treatments, including surgery, radiotherapy, targeted therapy, and immunotherapy, are administered alone or in combination.[4] Combination therapy is an efficient strategy for improving efficiency and reducing side effects associated with individual use.[5]

Doxorubicin hydrochloride (DOX), a chemotherapeutic drug, is a subclass anthracycline antibiotic.[6,7] DOX intercalates deoxyribonucleic acid (DNA) and suppresses DNA polymerase, thereby inhibiting DNA synthesis.[8] Although DOX is hydrophilic and is used to treat various cancers, its dangerous side effects, such as cardiac toxicity and photosensitivity, hinder its extensive use.[9]

One of a patient-friendly cancer therapy strategy is photodynamic therapy (PDT), because it is a non-surgical therapy.[10] PDT comprises three essential factors: a photosensitizer (PS) as a tumor-selective drug; oxygen; and light at specific wavelengths.[11] PS is photochemically associated with light, which induces singlet oxygen ($^1O_2$) as a reactive oxygen species (ROS). The generated ROS directly induces apoptosis or necrosis of tumor cells without affecting adjacent healthy cells.[12] As a result, these factors are not toxic but affect apoptosis-induced oxidative damage when combined. Currently, the available PDT is primarily classified into two categories: porphyrin and its derivatives as first-generation PSs, and chlorin and its derivatives as second-generation PSs. Second-generation PSs have a relatively long absorption wavelength compared with first-generation PSs, enabling easy penetration of light into the human body to target tumors deep in the tissues.[13,14] Purpurin-18 sodium salt (P18Na), a second-generation PS, is derived from chlorophyll and is hydrophilic.[14]

Despite the worthy combined therapy of PDT and/or chemotherapy to treat cancer, there are concerns regarding

Received: March 11, 2023
Accepted: April 7, 2023
Published: April 26, 2023

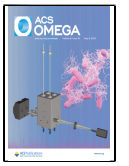

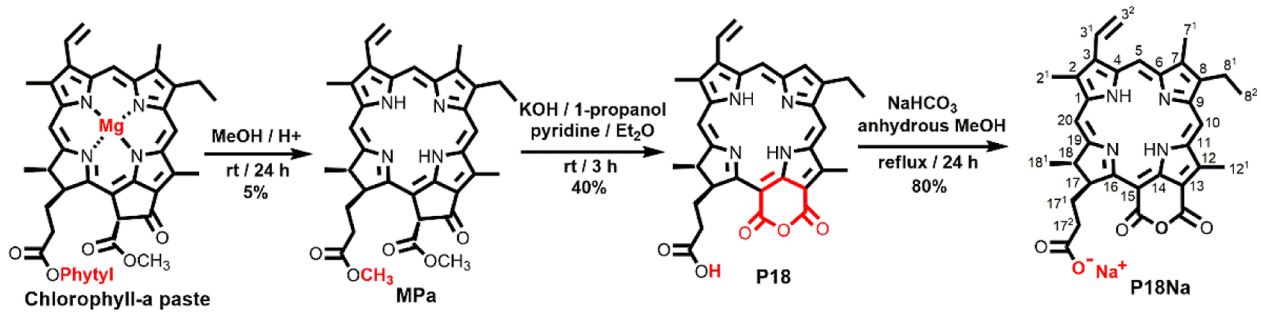

(A)

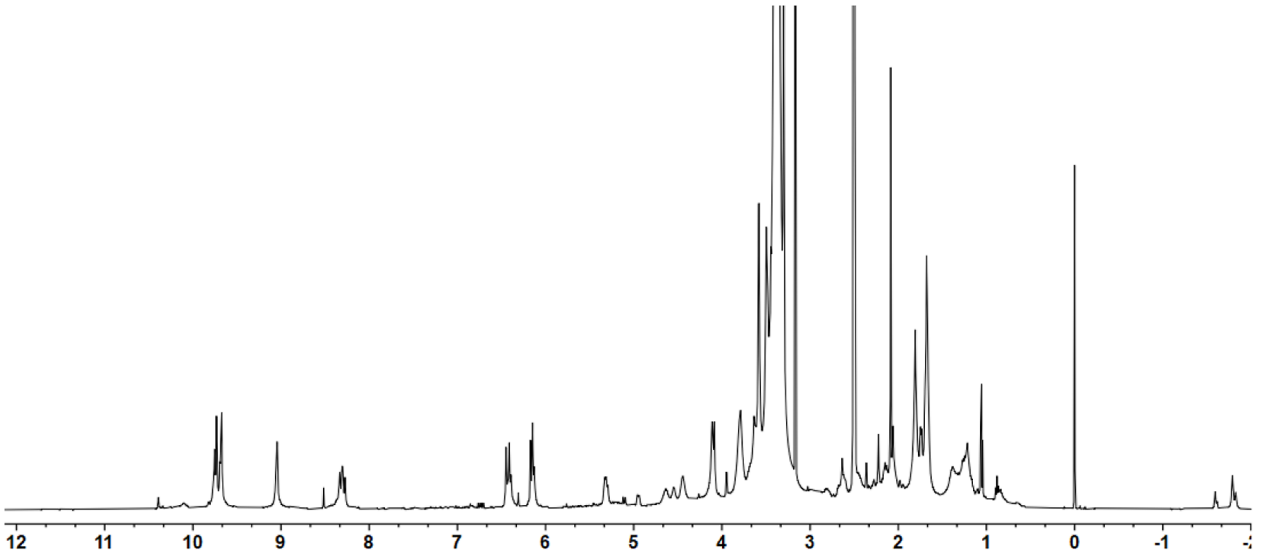

(B)

Figure 1. (A) Scheme for synthesis sequence of P18Na with numbering, (B) ^{1}H NMR spectrum of P18Na (500 MHz, $(CD_3)_2SO$, 25 °C, TMS). MPa, methyl pheophorbide-a; P18, purpurin 18; P18Na, purpurin 18 sodium salt.

instability of light, side effects, and significant hepatic first-pass metabolism.[9,15] Liposome systems are biocompatible lipid-based pH-responsive carriers that are largely applied to anti-cancer treatment.[6,16] The amphiphilic properties that are phospholipid properties effectively load hydrophilic drugs into the core of the liposome.[17,18] Transferosome, a liposome-class carrier system, is fabricated by employing an edge activator (EA) as a surfactant to provide a tight bilayer structure of liposome flexibility.[19,20] The flexibility of transferosomes is advantageous in passive targeting strategies for cancer treatment. According to the enhanced permeability and retention (EPR) effects of passive targeting, nanoparticles up to a size of 400 nm are passively retained at the tumor site.[3,21,22] As a result, transferosomes effectively permeate the leaky vasculature at the tumor site.[23]

In this study, DOX and P18Na were loaded into transferosomes as a combined pharmaceutical formulation to achieve effective cancer treatment using chemotherapy and PDT. P18Na is synthesized from chlorophyll, and its arrangement form was determined using ^{1}H nuclear magnetic resonance (^{1}H NMR) spectroscopy. The absorption wavelengths of P18Na and DOX were evaluated using UV−vis spectroscopy. The formulation properties of P18Na- and DOX-loaded transferosomes assessed via size, polydispersity index (PDI), and ζ potential. The pharmacological effects for the combined formulations were estimated via $^1O_2$ photogeneration as a non-biological assay using the 1,3-diphenylisobenzofuran (DPBF) assay. Further, the in vitro phototoxicity was investigated using two cancer cell lines (HeLa from human cervical and A549 from human lung carcinoma) via a biological assay.

RESULTS AND DISCUSSION

Characterization of P18Na. *NMR Spectroscopy.* ^{1}H NMR spectroscopy was conducted to determine the arrangement form of P18Na. Figure 1 shows the ^{1}H NMR spectrum of P18Na. ^{1}H NMR (500 MHz, DMSO-d_6, 25 °C, TMS): δ 9.73 (s, 1H, 10H), 9.67 (s, 1H, 5H), 9.04 (s, 1H, 20H), 8.34−8.27 (m, 1H, 3^1H), 6.45 (dd, J = 17.8 Hz, 1H, 3^2H), 6.17 (d, J = 11.5 Hz, 1H, 3^2H), 5.31 (m, 1H, 17H), 4.44 (m, 1H, 18H), 4.11 (m, 2H, 8^1H), 3.79 (br, 3H, 12^1H), 3.64 (s, 3H, 2^1H), one singlet (s, 3H, 7^1H) overlapped with DMSO water, 2.64 (m, 1H, 17^2H), 2.45 (m,

https://doi.org/10.1021/acsomega.3c01654
ACS Omega 2023, 8, 16479−16490

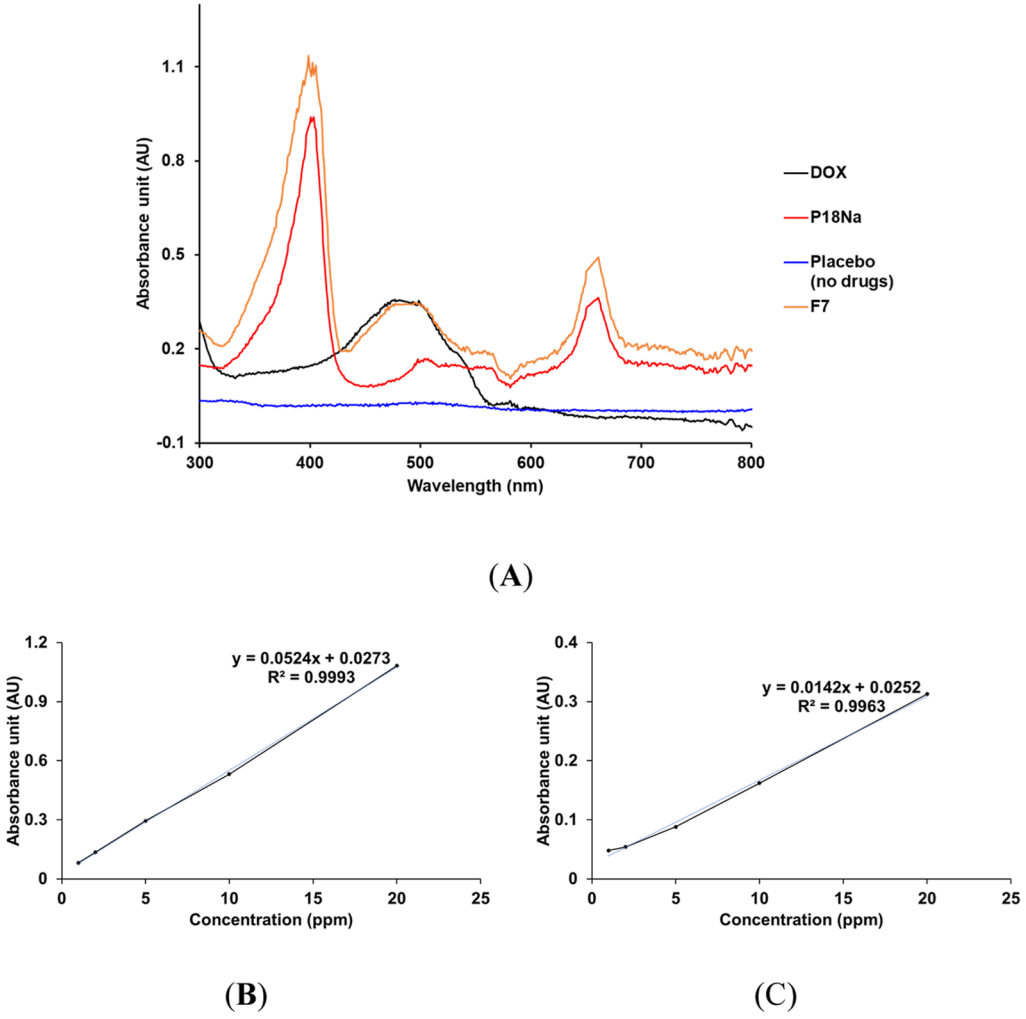

Figure 2. Calibration curves and UV−vis spectra of P18Na and DOX. (A) Specificity for P18Na, DOX, placebo, F7 (P18Na- and DOX-loaded transferosome) (DW, 25 °C). (B) Linearity for P18Na, and (C) DOX standard stock solution in DW.

2H, 17^1H, overlapped with DMSO), 2.15 (m, 1H, 17^2H), 1.81 (m, 3H, 18^1H), 1.68 (t, J = 7.2 Hz, 3H, 8^2H), and −1.59 and −1.79 (all brs and each 1H, NH). The peak for the proton signal of −COOH in P18 at 12.02 ppm disappeared, confirming the formation of the carboxylate sodium salt, P18Na.

Preparation of the Analytical Method for P18Na and DOX. An analytical method was developed to determine P18Na and DOX. A UV−vis spectrophotometer was used to record the optical absorption spectrum in the range of 300 to 800 nm; the maximum wavelength and specific spectra were identified.[24] Figure 2 shows the UV−vis spectra of P18Na and DOX at 661 and 495 nm, respectively. The results for the placebo transferosome (formulation without two drugs) revealed no interference between the placebo and analyte.

Two calibration curves for P18Na and DOX were prepared for each of the prepared stock solutions, with concentrations ranging from 1 to 20 ppm. According to linear regression analysis, the correlation coefficients for P18Na and DOX were 0.9993 and 0.9963, respectively, as shown in Figure 2.

The proximity of the measured values to the same concentration of each standard stock solution was determined. Precision of repeatability is exhibited as the RSD. Table 1 shows the precision results for P18Na and DOX, which were 0.28 and 1.68%, respectively, ultimately confirming the high precision of the prepared analysis.

Table 1. Precision for the Stock Solutions of P18Na and DOX Obtained from the Prepared Analysis

	recovery (%)	
no	P18Na	DOX
1	99.66	103.41
2	100.34	100.00
3	100.00	100.00
4	100.34	101.14
5	100.00	101.14
6	99.66	104.55
average (%)	100.00	101.70
SD (%)	0.28	1.70
RSD (%)	0.28	1.68

To assess the closeness of accordance between the test substances and a typical true, accuracy is expressed as an RSD by calculating the drug recovery. The accuracy results for P18Na and DOX were 0.57, 0.28, and 0.19% for P18Na and 0.98, 1.40, and 0.66%, respectively, as shown in Table 2. Such findings confirm the high accuracy of the prepared analysis.

Preparation and Characterization of P18Na- and COX-Loaded Nano-Transfersomes. *Preparation Method.* P18Na- and DOX-loaded nano-transfersomes were prepared by mixing of P18Na, DOX, lipid (lecithin), membrane stabilizer

https://doi.org/10.1021/acsomega.3c01654
ACS Omega 2023, 8, 16479−16490

Table 2. Accuracy for the Stock Solutions of P18Na and DOX Obtained from the Prepared Analysis

		recovery (%)		average (%)		SD (%)		RSD (%)	
drug (ppm)	No	P18Na	DOX	P18Na	DOX	P18Na	DOX	P18Na	DOX
1	1	101.22	102.08	100.41	100.69	0.57	0.98	0.57	0.98
	2	100.00	100.00						
	3	100.00	100.00						
5	1	100.34	103.41	100.00	101.52	0.28	1.42	0.28	1.40
	2	100.00	101.14						
	3	99.66	100.00						
20	1	100.46	98.72	100.22	99.57	0.19	0.66	0.19	0.66
	2	100.18	99.68						
	3	100.00	100.32						

(cholesterol), and edge activators (SP 20 and TW 80) through the probe sonication method, resulting in various formulations (F1−F8). The various compositions for the formulations of P18Na- and DOX are summarized in Table 3.

Table 3. Composition of the P18Na- and DOX-Loaded Nano-Transferosomes[a]

	drug (mg)		lipid (mg)	membrane stabilizer (mg)	edge activator (mg)	
formulation	P18Na	DOX	lecithin	cholesterol	SP 20	TW 80
F1	10		600			
F2	10		600	200		
F3	10		600		200	
F4	10		600			200
F5	10		600	200	200	
F6	10		600	200		200
F7	5	5	600	200		200
F8		10	600	200		200

[a]P18Na, purpurin-18 sodium salt; DOX, doxorubicin hydrochloride; SP 20, Span 20; TW 80, Tween 80.

Determination of Nano-Particle Size, Polydispersity Index (PDI), and ζ Potential. In cancer therapy, particle size is a significant parameter based on the EPR effect and cellular uptake.[25] ζ potential ensures particle stability in a nanoparticle, and causes a repulsive force induced by the electric surface potential on particles. Particles with high ζ potentials prevent coalescence.[26] Figure 3 shows the results of particle characterization of P18Na and DOX-loaded transferosomes. The sizes, PDTs, and ζ potentials of all formulations were 98.38−217.50 nm, 0.25−0.36, and −23.63−−41.10 mV, respectively. In liposomes, F1 had a smaller particle size and lower ζ potential than F2, which contains cholesterol. Such finding suggests that cholesterol enhances the stability by reinforcing the phospholipid bilayer.[16,27] Based on the effects of EA, F3 and F5 using SP 20 as a lipophilic EA had higher particle size and ζ potential values, while F4 and F6 using TW 80 as hydrophilic EA had smaller particle sizes and lower ζ potentials. Such finding suggests that lipophilic or hydrophilic EA could reinforce the lipid bilayer or drug-entrapped aqueous core in transferosomes, respectively. Accordingly, the reinforced lipid bilayer significantly increases the size and ζ potential for the nano-transferosomes.[18,20]

Determination of the Entrapment Efficiency (EE) and Loading Amount (LA). EE and LA are significant parameters in the nanodrug delivery systems as they avoid side effects, enhance entrapped drug stability, and prevent hepatic first-pass metabolism by delivering drugs into the lymph.[21,28−30] As

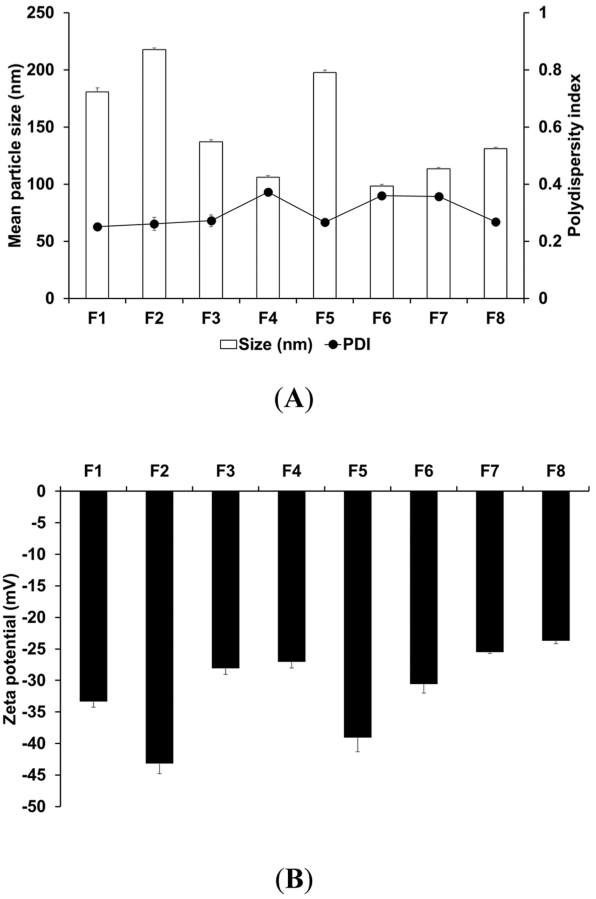

Figure 3. Particle properties of average data for (A) particle size and PDI and (B) ζ potential of the P18Na- and DOX-loaded nano-transferosomes. Results are exhibited as the mean ± standard deviation for the triplicate (n = 3). PDI, polydispersity index.

shown in Figure 4, the loading capacity results for the formulations entrapping P18Na were 43.80−63.03% (EE) and 0.52−1.04% (LA), while the results for those entrapping DOX were 46.57−54.13% (EE) and 0.55−0.77% (LA), respectively. The order of the EE and LA of P18Na from F1 to F4 was F4 > F3 > F2 > F1. This suggests that P18Na, as a hydrophilic drug, was entrapped in the aqueous core of the transferosomes. Thus, the formulation with high hydrophilicity (F4) had the highest P18Na EE; this was also observed in F5 and F6. F3 and F4, without cholesterol, had relatively higher EE than F5 and F6 containing cholesterol; this is due to the hydrophilic properties of P18Na and the lipophilic properties of cholesterol.

https://doi.org/10.1021/acsomega.3c01654
ACS Omega 2023, 8, 16479−16490

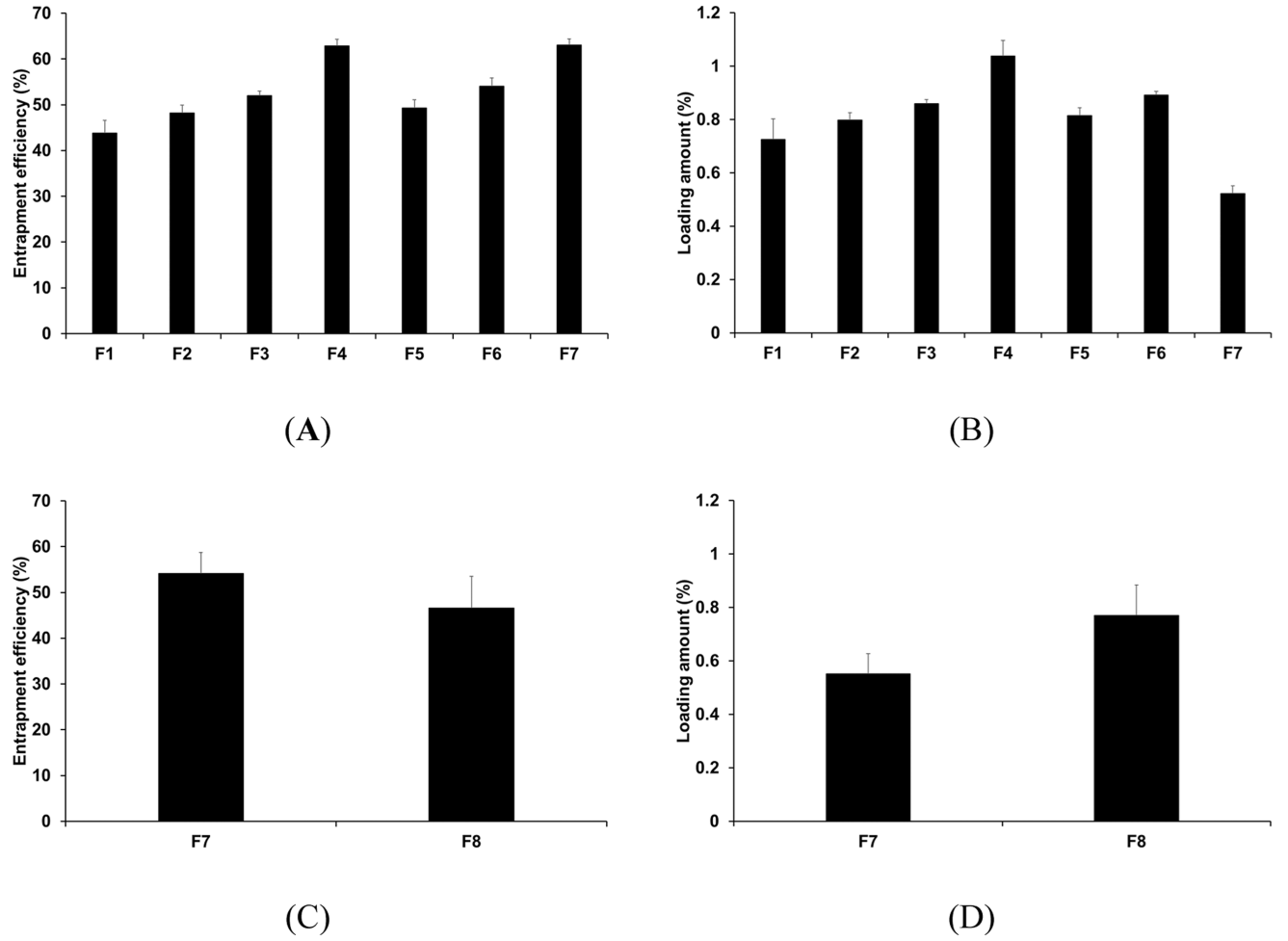

Figure 4. EE and LA of P18Na- and DOX-loaded nano-transferosomes. Results are exhibited as mean ± standard deviation for triplicate ($n = 3$). (A) Entrapment efficiency (EE) and (B) loading amount (LA) of P18Na in the nano-transferosomes. (C) EE and (D) LA of DOX in the nano-transferosomes. P18Na, purpurin 18 sodium salt; DOX, doxorubicin.

In Vitro P18Na and DOX Release Studies. The release profiles of P18Na and DOX from P18Na- and DOX-loaded nano-transferosomes were determined using the dialysis membrane method. Particularly, both pH 7.4 and pH 5 conditions were conducted because transferosomes, which act as a liposome system, are pH-sensitive formulations, and the drug release profiles were determined in a simulated environment for the human body (pH 7.4) and cancer cells (pH 5). As shown in Figure 5, the amount of P18Na released after 48 h was F1 > F4 > F3 > F2 > F7 > F6 > F5. For P18Na, F4 using TW 80 was faster than F3 and F2 using SP 20 and cholesterol, respectively; this could be related to the lower particle stability corresponding to the lower ζ potential of F4. It is more difficult for the drug entrapped in the nanoparticle with high stability to migrate out of the particle than that in the relatively unstable particle.[30] The release of P18Na and DOX at pH 7.4 was 14.35−23.77% and 18.10−22.78% after 48 h, respectively, which reveals typical sustained drug release. However, at pH 5, P18Na and DOX release showed pH-responsive burst release until 12 h, followed by sustained release until 24 h to reach approximately 100% release (4−6-fold faster than those at pH 7.4) in all formulations, except DOX release in F7, which showed very slow sustained release to reach 100% at 48 h. This result could be attributed to lecithin as the main ingredient. Lecithin, one of the phospholipids, is easily decomposed in acidic conditions due to its pH-sensitivity.[31] This study was meaningful as transferosomes might be transferred into tumor sites without drug escape in the body, and the entrapped drugs are rapidly released after cellular uptake.

Drug Release Kinetics Models. The drug release results were analyzed with kinetics models (zero order, first order, Higuchi, and Korsmeyer-Peppas). Table 4 shows that the correlation coefficient (R^2) value of the Higuchi model was the highest.[32] This suggests that the release of P18Na and DOX from nano-transferosomes was based on diffusion and dissolution. Additionally, those drugs were entrapped homogeneously in the entire matrix of nano-transferosome.[32,33]

Stability for Light. The photostability of P18Na and DOX, which are light-induced therapies and light-sensitive drugs, respectively, is of great concern for storage. As depicted in Figure 6, the photostability results of P18Na and DOX revealed that all formulations improved the photostability of both drugs with different abilities. After 40 min of irradiation, the percentages of the remaining P18Na and DOX from these solutions and all formulations were 74.42 and 80.15%−96.42%, and 81.40 and 95.50%−96.68%, respectively. Regarding the effect of EA, F3 and F5 with SP 20 effectively protected P18Na from light compared to F4 and F6 with TW 80; this is because highly stable particles can entrap a large amount of drug, which effectively protects the entrapped drug from light.[34]

https://doi.org/10.1021/acsomega.3c01654
ACS Omega 2023, 8, 16479−16490

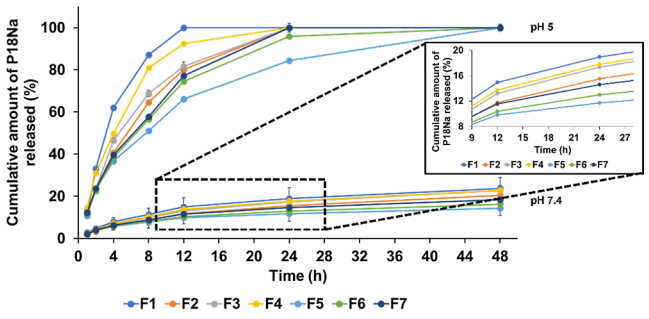

(A)

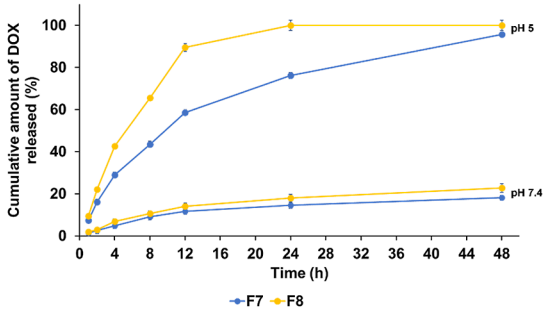

(B)

Figure 5. Cumulative percentage release profiles of (A) P18Na and (B) DOX from transferosomes in the release medium. Results are expressed as the mean ± standard error for triplicate (n = 3).

$^1O_2$ Photogeneration. The efficacy of P18Na in PDT was evaluated using the DPBF assay, a non-biological assay. The intensity of DPBF decreased as the $^1O_2$ generated following photoirradiation of P18Na reacted with DPBF. MB, a standard $^1O_2$ sensitizer, was treated with a PC. The percentages of DPBF intensity for MB, P18Na, and the nano-transferosomes were 49.29, 87.75, and 60.08%−71.15%, respectively, as shown in Figure 7. All formulations had a better $^1O_2$ photogenerating efficacy than P18Na. The PDT efficacy of P18Na was improved via entrapping in nano-transferosomes. This finding suggests that the nanonized transferosomes indirectly improved PDT efficacy by preventing the coalescence of P18Na.[30] Regarding the reduced efficacy according to the increase in particle stability in F1−F4, the unstable particles had a low EE, which is a large amount of non-entrapped P18Na. This vulnerable P18Na was exposed to relative light. Owing to the biological side effects, the efficacy of PDT must be evaluated in targeted cells.

In Vitro Cytotoxicity Studies. The cytotoxicity of P18Na and DOX to HeLa (cervical carcinoma originated from humans) and A549 (lung epithelial carcinoma originated from humans) was evaluated using the WST assay. As shown in Figure 8, the cytotoxicity under dark conditions was used to determine the safety of the test substances in PDT, whereas that under light conditions was due to PDT efficacy. To obtain the inhibitory medium concentration values (IC_{50}), each sample was tested at different concentrations (1, 2.5, 5, and 10 μM), as summarized in Table 5. The cytotoxicity results obtained in the dark revealed that all formulations, except the DOX-loaded transferosomes, were non-irritant. The results of light cytotoxicity revealed irritation for all test substances. Such finding suggests that DOX, as a chemotherapy drug for cancer treatment, induced its anti-cancer efficiency regardless of photoirradiation, whereas P18Na, as a PDT drug, was safe unless otherwise irradiated.[35]

The IC_{50} results showed that the order of anti-cancer efficacy was the same in both cell lines as outlined below: F7 (0.66 μM) > F6 (0.70 μM) > F1 (0.72 μM) > F5 (0.77 μM) > F2 (0.80 μM) > F8 (0.90 μM) > P18Na (0.95 μM) > DOX (1.72 μM) in HeLa cells; and F7 (0.63 μM) > F6 (0.69 μM) > F1 (0.71 μM) > F5 (0.72 μM) > F2 (0.78 μM) > F8 (0.83 μM) > P18Na (0.89 μM) > DOX (1.90 μM) in A549 cells. This finding suggests that the enhanced anticancer efficacy could be attributed to the particle size effect based on the EPR effect.[28,36] Accordingly, F1, which has a relatively small particle size and low EE, has a higher anticancer efficacy than F2, which has a relatively large particle size and high EE. Therefore, in this study, the anti-cancer efficacy confirmed that it dominates particle size rather than EE,

Table 4. Correlation Coefficient (R^2) Values for the in vitro Release Profiles Fitted with Multiple Drug-Release Kinetics

			correlation coefficient (R^2) values of drug-release kinetics			
drug	formulations		zero order	first order	Higuchi	Korsmeyer-Peppas
P18Na	pH 7.4	F1	0.831	0.858	0.978	0.871
		F2	0.872	0.893	0.989	0.930
		F3	0.867	0.890	0.988	0.914
		F4	0.854	0.879	0.985	0.897
		F5	0.774	0.791	0.957	0.878
		F6	0.813	0.832	0.973	0.900
		F7	0.831	0.852	0.979	0.895
	pH 5	F1	0.478	0.634	0.743	0.615
		F2	0.670	0.847	0.890	0.667
		F3	0.639	0.846	0.869	0.677
		F4	0.554	0.814	0.809	0.613
		F5	0.794	0.989	0.963	0.688
		F6	0.724	0.971	0.923	0.687
		F7	0.701	0.846	0.907	0.677
DOX	pH 7.4	F7	0.820	0.839	0.962	0.950
		F8	0.836	0.861	0.972	0.928
	pH 5	F7	0.842	0.996	0.977	0.768
		F8	0.626	0.833	0.854	0.703

https://doi.org/10.1021/acsomega.3c01654
ACS Omega 2023, 8, 16479−16490

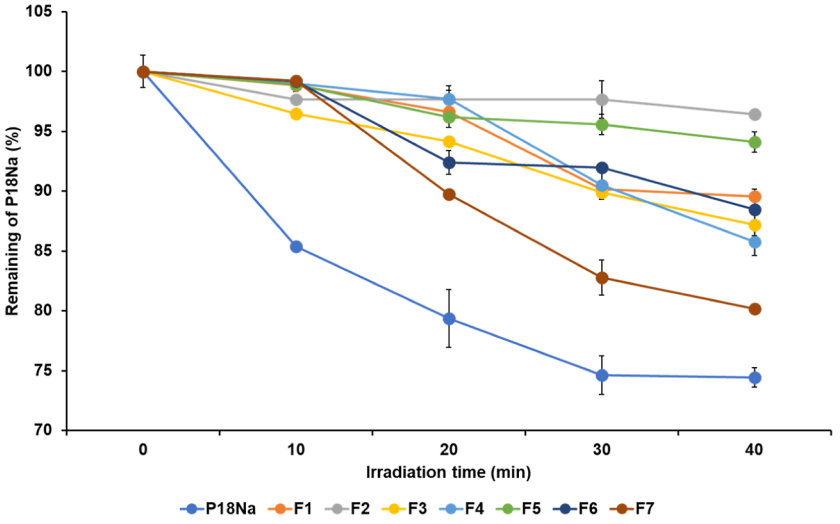

(A)

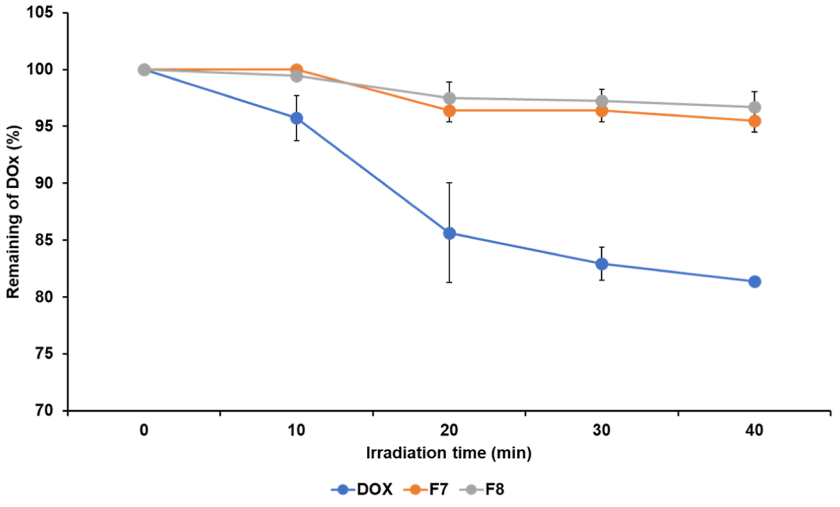

(B)

Figure 6. Photostability for the non-degraded (A) P18Na and (B) DOX from drug solutions and P18Na- and DOX-loaded transferosomes before and after irradiation with LED. Results are expressed as mean ± standard deviation for triplicate (n = 3).

based on the EPR effect and easy cellular uptake. Further, the order of cancer cell apoptosis for F6 (P18Na-loaded formulation) and F8 (DOX-loaded formulation) was similar to that of P18Na and DOX. Such finding suggests that the anticancer effect of P18Na (PDT) is more efficient than that of DOX (chemotherapy). In particular, based on the anti-cancer effect of F7, the combination of chemotherapy and PDT had the greatest anti-cancer effects among the tested substances in HeLa and A549 cell lines. These results reveal that the combination of chemotherapy and PDT for cancer treatment is more efficient than individual use. The combination index (CI) values between P18Na and DOX that are P18Na&DOX and F7 demonstrated all antagonism.

■ CONCLUSIONS

In this study, we synthesized P18Na- and DOX-loaded nano-transferosomes as a combination of PDT and chemotherapy for the treatment of cancer. The synthesized P18Na was identified by ^{1}H NMR, in which all proton signals were fully assigned, confirming successful synthesis. The particle sizes and ζ potentials of the formulations were 98.38−217.50 nm and −23.63−−41.10 mV, respectively. All formulations displayed pH-responsive release, with sustained drug release in pH 7.4 and burst release in pH 5. This result implies that P18Na- and DOX-loaded nano-transferosomes were effectively delivered into cancer cells with less drug escape in the body. Thereafter, both drugs were released in a pH-responsive manner in cancer cells, enabling sufficient therapeutic activity using photodynamic/chemo combination therapy. The photostability of DOX as a photosensitive drug and P18Na as a light-induced therapy was improved by entrapping DOX into nano-transferosomes. Further, photocytotoxicity studies using HeLa and A549 cell lines revealed a size-dependent anti-cancer effect. Therefore, nano-transferosomes containing P18Na and DOX are consid-

https://doi.org/10.1021/acsomega.3c01654
ACS Omega 2023, 8, 16479−16490

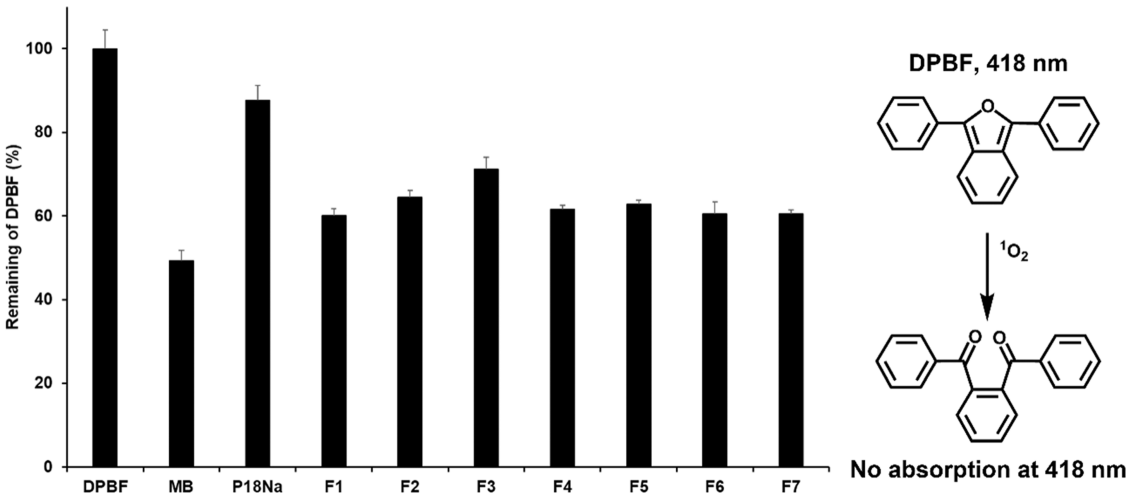

Figure 7. DPBF absorbance decay (%) for P18Na with/without transferosomes at 418 nm after photoirradiation (total light dose 2 J/cm^2; irradiation time 15 min). Results are expressed as mean ± standard deviation for triplicate (n = 3). NC: DPBF (1,3-diphenylisobenzofuran); PC: MB (methylene blue); P18Na (purpurin-18 sodium salt). Statistical significance between the P18Na solution and the formulations is stated by a single asterisk (p < 0.05) or double asterisks (p < 0.01).

ered effective cancer treatment when administered as a photodynamic and chemo combination therapy.

EXPERIMENTAL SECTION

Materials. Lecithin was purchased from Now Foods (Bloomingdale, IL, USA). PBS, MB, and DOX were obtained from Sigma-Aldrich (St. Louis, MO, USA). Cholesterol, acetone, and dimethyl sulfoxide (DMSO) were supplied by SAMCHUN (Pyeongtaek, Korea). SP 20 and TW 80 were obtained from Dae Jung Co. Ltd. (Busan, Korea). Chlorophyll-a paste was obtained from Shandong Lanmo Biotech Co. Ltd. (Shanghai, China). MC (CH_2Cl_2) was purchased from Duksan Co. Ltd. (Gyeonggi-do, Korea). DPBF was purchased from TCI Chemicals (Tokyo, Japan). DMEM was supplied by WelGENE (Gyeongsan, South Korea). Penicillin−streptomycin solution (100 ×) and FBS were purchased from BioWest (Nuaillé, France). The cancer cell lines (HeLa and A549) were obtained from the Korea Cell Line Bank (Seoul, Korea). The Quanti-MAX WST-8 assay kit was purchased from Biomax (Seoul, Republic of Korea). High-performance liquid chromatography (HPLC) grade methanol (MeOH) was purchased from Honeywell (Seelze, Germany). All other chemicals were of HPLC grade.

Synthesis of P18Na. MPa was synthesized from chlorophyll-a paste based on a previously reported procedure.[37] Pyridine, diethyl ether, and KOH were dissolved in 1-propanol, and then MPa (1 g) was added and stirred under aeration conditions for 3 h. The resultant was poured to DW. Thereafter, the obtained organic layer was evaporated. The residue was separated by column chromatography using 5% MeOH/MC as the eluent. Pure P18 was dissolved in MC with $NaHCO_3$ and MeOH, and stirred under reflux for 24 h, affording P18Na after crystallization from an excess amount of $NaHCO_3$.

Preparation of P18Na and DOX-Loaded Nano-Transferosomes. P18Na- and DOX-loaded nano-transferosomes were prepared by sonication. Briefly, P18Na, DOX, and lecithin were added in MC with or without cholesterol and EA (SP 20 and TW 80). A thin lipid film was formed by removing MC using a rotary vacuum evaporator. To prepare the transferosomes, the obtained thin lipid film was hydrated via the addition of DW and sonicated using K410HTD (Shenzhen Guan Yijia Technology Co., Ltd., Shenzhen, China). The fabricated transferosomes were ultrasonicated by Scientz-IID, (Ningbo, China) as a probe sonicator at 300 W for 15 min, with a 5 s pulse-on period and a 5 s pulse-off period. The effects of the various compositions of P18Na- and DOX-loaded nano-transferosomes were investigated, as presented in Table 3.

Characterization of P18Na and DOX. *NMR Spectroscopy of P18Na.* ^{1}H NMR was proceeded by a Varian spectrometer [500 MHz, $(CD_3)_2SO$] at the Biohealth Products Research Center of Inje University.

Preparation of the Analytical Method for P18Na and DOX. The concentrations of P18Na and DOX were measured using a UV−vis spectrophotometer (S-3100; Scinco, Seoul, Korea) at ambient temperature. To determine the maximum absorption wavelength of P18Na and DOX, the absorption spectrum of P18Na and DOX was measured in the wavelength range of 300−800 nm. The solvent was used MeOH due to the most highly characteristics for this method. Accordingly, to prepare a standard stock solution, 2 mg of an accurate amount of each drug was added in 20 mL of MeOH.

To determine a five-point linearity, the final concentrations of 1−20 ppm were obtained by diluting the stock solution. Stock solutions of various concentrations were prepared. Calibration curves and concentration versus absorbance units were derived for each drug.

The precision of the developed method was established by conducting an assay with six replicate determinations of the sample preparation at test concentrations. RSD from the results was also calculated.

To determine the accuracy, recovery was carried out by adding a known quantity of the standard to the pre-analyzed sample. The recovery was used at 0, 25, and 100% levels, and the contents were quantified from the respective UV−vis absorption spectra.

Characterization of the P18Na- and DOX-Loaded Nano-Transferosomes. *Determination of Nano-Particle Size, PDI, and ζ Potential.* The size and PDI of the formulations were determined at 25 °C using a Zetasizer Nano ZS (Malvern Instruments Ltd., Worcestershire, Malvern, UK). The ζ potential of the nano-transferosomes was estimated using a Zetasizer Nano ZS. The test substances were diluted 10-fold

https://doi.org/10.1021/acsomega.3c01654
ACS Omega 2023, 8, 16479−16490

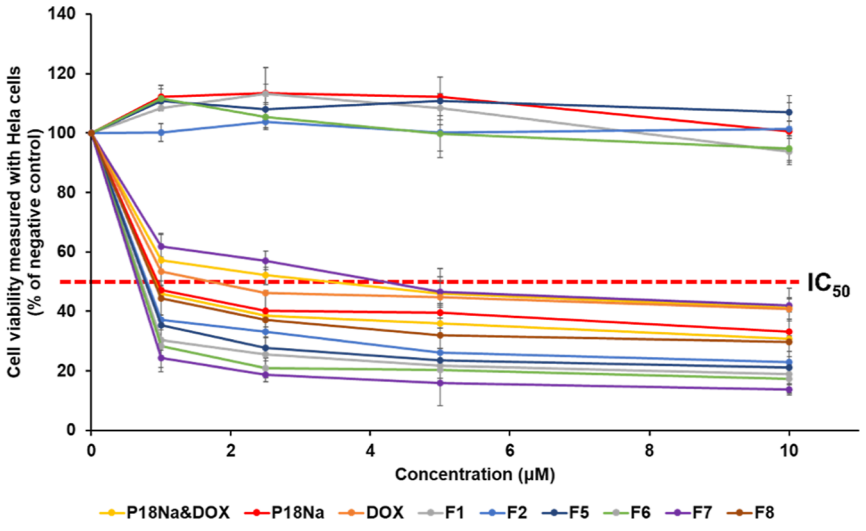

(A)

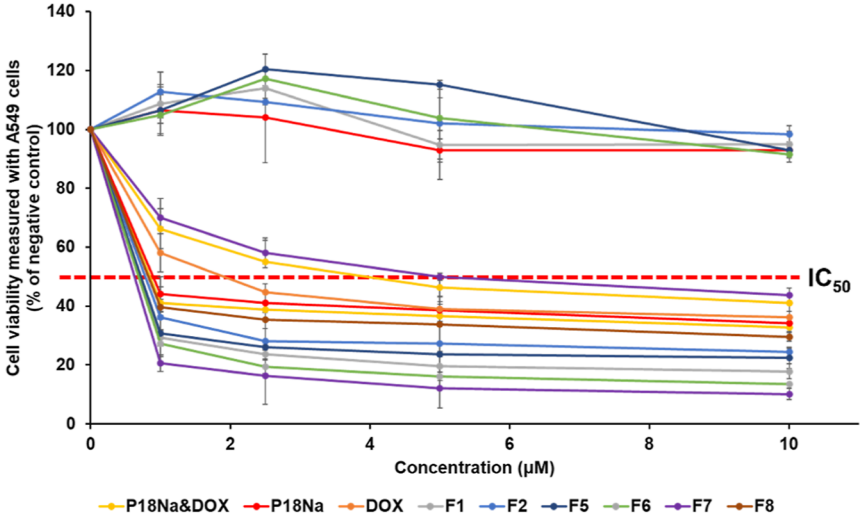

(B)

Figure 8. Cytotoxicity for the pure solutions of P18Na, DOX, and P18Na&DOX, F1, F2, F5, F6, F7, and F8 applied to HeLa and A549. Estimation of viability was to use the WST assay. Cytotoxicity of (A) HeLa cells and (B) A549 cells in both dark and light conditions. Results are exhibited as mean ± standard deviation for triplicate (n = 3).

Table 5. IC_{50} and CI Values in HeLa or A549 Cells, Particle Size, and Entrapment Efficiency (EE) of the Pure Solutions of P18Na, DOX, and P18Na&DOX, F1, F2, F5, F6, F7, and F8[a]

	Hela (μM)		A549 (μM)			EE (%)	
	IC_{50}	CI at IC_{50}	IC_{50}	CI at IC_{50}	particle size (nm)	P18Na	DOX
P18Na	0.95		0.89		N/A	N/A	N/A
DOX	1.72		1.90		N/A	N/A	N/A
P18Na &; DOX	0.92	1.50	0.85	1.40	N/A	N/A	N/A
F1	0.72		0.71		180.73 ± 3.32	43.80 ± 2.76	N/A
F2	0.80		0.78		217.50 ± 1.50	48.22 ± 1.74	N/A
F5	0.77		0.72		197.57 ± 2.19	49.27 ± 1.80	N/A
F6	0.70		0.69		98.38 ± 1.34	54.02 ± 1.82	N/A
F7	0.66	1.68	0.63	1.67	113.40 ± 1.21	63.03 ± 1.36	54.13 ± 4.65
F8	0.90		0.83		130.97 ± 1.03	N/A	46.57 ± 6.97

[a]N/A, not applicable.

https://doi.org/10.1021/acsomega.3c01654
ACS Omega 2023, 8, 16479−16490

with DW. Each value represents the average of three measurements.

Determination of EE and LA. The EE and LA of P18Na- and DOX-loaded transferosomes were determined by centrifugation. The prepared formulations were diluted 10-fold. The resultant was then centrifuged at 1300 rpm for 1 h at 4 °C. The concentration of non-encapsulated drug in the supernatant was quantified using a UV−vis spectrophotometer. EE and LA were estimated by eqs 1 and 2, respectively.

$$\text{EE}\ (\%) = [(\text{Amount of total drug} - \text{Amount of nonencapsulated drug})/(\text{Amount of total drug})] \times 100 \quad (1)$$

$$\text{LA}\ (\%) = \{[\text{Amount of total drug} - \text{Amount of nonencapsulated drug}]/[(\text{Amount of total drug} - \text{Amount of nonencapsulated drug}) + \text{Amount of lipid}]\} \times 100 \quad (2)$$

In Vitro P18Na and DOX Release Studies. The in vitro release studies for P18Na and DOX were carried out by the dialysis bag method. A predetermined amount of each test substance was soaked in the dialysis bags (Spectrum Laboratories, Inc., Compton, CA, USA) with a molecular weight of 10 kDa. The sealed bags were placed in 70 mL vials with 50 mL of receptor medium (PBS, pH 7.4), followed by shaking at 100 rpm and 37 ± 0.5 °C in a shaking incubator (JSSI-100T, JS Research Inc., Gongju, Korea). 1 mL of receptor medium was withdrawn from the vial at 1, 2, 4, 8, 12, 24, and 48 h. Thereafter, the withdrawn samples were passed through 0.45 μm membrane filters (SFCA Syringe Filters, Corning Inc., NY, USA) to be quantified.

Drug Release Kinetics Models. To elucidate the mechanism of P18Na and DOX releases from the nano-transferosomes, the P18Na and DOX release profiles of the nano-transferosomes were analyzed with various models of release kinetics, including zero-order, first-order, Higuchi, and Korsmeyer-Peppas models using eqs 3−6, respectively.[32,33]

$$Q_t = K_0 t + C_0 \quad (3)$$

$$\log C = \log C_0 - K_t/2.303 \quad (4)$$

$$Q_t = K_H t^{1/2} \quad (5)$$

$$Q_t = \mathrm{K}t^n \quad (6)$$

Where Q_t is the drug release amount at time t, Q_0 is the initial drug amount in formulations, K_0, K_t, K_H are release rate constants, and C_0 is the initial concentration of the drug.

Stability for Light. The stability of P18Na and DOX for light in the nano-transferosomes was determined via a comparison with P18Na or DOX in a 0.1% MeOH solution. The photostability of P18Na and DOX was monitored by recording their absorption spectra at wavelengths of 661 and 495 nm, respectively. Briefly, 20 mL of P18Na, DOX, or P18Na- and DOX-loaded nano-transferosomes in a 0.1% MeOH solution (4.0 ppm) was irradiated (2 J/cm^2) with LED at different time intervals (0, 10, 20, 30, and 40 min). P18Na and DOX were then withdrawn from the formulations by melting the lipids caused by hexane. A MeOH layer with the withdrawn drugs was filtered through 0.22 μm filters to be quantified.

$^1O_2$ Photogeneration. The $^1O_2$ photogeneration study was performed using DPBF. DPBF, a selective $^1O_2$ acceptor, is bleached upon reaction with $^1O_2$, leading to a reduction for the DPBF absorption. Each sample (1 μM) with 50 μM of DPBF in DMSO was used to evaluate photogeneration. The negative control (NC) and positive control (PC) contained 50 μM DPBF and 1 μM MB with 50 μM DPBF, respectively. All test substances prepared in the dark were located in a 48-well plate and covered with an aluminum foil. The plate was irradiated (2 J/cm^2) with LED for 15 min. The DPBF absorption was estimated at 418 nm with Synergy HTX (BioTek, Winooski, VT, USA) as a microplate reader.

In Vitro Cytotoxicity Studies. *Cytotoxicity Study Using a Human Tumor Cell.* The cancer cell death efficacy of P18Na and DOX in a combined therapy of PDT and chemotherapy was carried out. Two cell lines [cervical carcinoma originated from human (HeLa) and lung carcinoma originated from human (A549)] were seeded in 48-well plates at 2 × 10^4 cells/well. The calculation of cell number was a hemocytometer method. The seeded cells were carried out incubation for 24 h at 37 ± 0.5 °C with 5% CO_2. Different concentrations (1, 2.5, 5, and 10 μM) of test substances were applied to each well, followed by exposure for 24 h. After rinsing the exposed cells by a sterile PBS. Thereafter, 200 μL of the growth medium was added to each well. The cells were then irradiated (2 J/cm^2) with LED at a distance of 20 cm for 15 min. After post-incubation for 24 h, WST assay was conducted.

Viability of Cancer Cells. Viability of cells was estimated by measuring the dehydrogenase activity of viable keratinocytes at 24 h after incubation.[38] A 10% WST solution was added to each well. After 1 h of reaction, the WST absorption was estimated at 450 nm with a microplate reader.

All experiments were experimented for triplicate. After subtracting the blank OD from all raw data, viability was estimated using the percentage of cell viability relative to that of the NC was expressed using eq 7. The NC value was set at 100%.

$$\text{Viability}\ (\%) = \frac{\text{Mean OD}_{\text{treated}}}{\text{Mean OD}_{\text{control}}} \times 100 \quad (7)$$

The CI was also calculated using eq 8 to evaluate the synergy of P18Na and DOX, according to the equation reported by Chou, T. C.[39]

$$\text{CI} = \frac{(D)_1}{(D_x)_1} + \frac{(D)_2}{(D_x)_2} \quad (8)$$

When the drug effect x % was obtained in combination treatment, $(D)_1$ and $(D)_2$ exhibit the concentrations of drugs 1 and 2, respectively. When the same drug effect was acquired in monoadministration, $(D_x)_1$ and $(D_x)_2$ exhibit the concentration of drugs 1 and 2, respectively. The assessment result of CI was an additive effect (CI = 1), synergism (CI < 1), and antagonism (CI > 1).

Statistical Analysis. The triplicate experiments were conducted for all analyses. The data (mean ± SD) were compared using one-way analysis of variance and Student's t-tests. Statistical significance was set at $p < 0.05$.

AUTHOR INFORMATION

Corresponding Authors

Sooho Yeo − *Center for Nano Manufacturing and Department of Nanoscience and Engineering, Inje University, Gimhae 50834, South Korea; Yonsei Institute of Pharmaceutical*

https://doi.org/10.1021/acsomega.3c01654
ACS Omega 2023, 8, 16479−16490

Sciences, Incheon 21990, Republic of Korea; College of Pharmacy, Yonsei University, Incheon 21990, Republic of Korea; orcid.org/0000-0002-6046-3168; Phone: +82-32-749-4173; Email: sooho32@hanmail.net; Fax: +82-32-479-4518

Il Yoon − *Center for Nano Manufacturing and Department of Nanoscience and Engineering, Inje University, Gimhae 50834, South Korea;* orcid.org/0000-0002-8562-1505; Phone: +82-55-320-3871; Email: yoonil71@inje.ac.kr; Fax: +82-55-321-7034

Woo Kyoung Lee − *Center for Nano Manufacturing and Department of Nanoscience and Engineering, Inje University, Gimhae 50834, South Korea*; Phone: +82-55-320-3875; Fax:; Email: wlee@inje.ac.kr; Fax: +82-55-320-3875

Author

Min Je Kim − *Center for Nano Manufacturing and Department of Nanoscience and Engineering, Inje University, Gimhae 50834, South Korea*

Complete contact information is available at: https://pubs.acs.org/10.1021/acsomega.3c01654

Author Contributions

Conceptualization: S.Y., I.Y., and W.K.L.; methodology: S.Y. and M.J.K.; resources: I.Y. and W. K. L.; writing-original draft preparation: S.Y.; funding acquisition: W.K.L.; supervision: W.K.L. All authors have read and agreed to the published version of the manuscript.

Notes

The authors declare no competing financial interest.

■ ACKNOWLEDGMENTS

This research was supported by the BK21 FOUR (Fostering Outstanding Universities for Research, no.5199991614715), the National Research Foundation of Korea (NRF) grant, the Basic Science Research Program through the National Research Foundation of Korea (NRF) funded by the Ministry of Education (MOE, Korea, NRF-2020R1I1A1A01060632), and the Korean government (MSIT) (NRF-2020R1F1A1070571). This research was supported by the Basic Science Research Program through the National Research Foundation of Korea (NRF) funded by the Ministry of Education (2018R1A6A1A03023718).

■ ABBREVIATIONS USED

P18Na, purpurin-18 sodium salt; DOX, doxorubicin hydrochloride; PDT, photodynamic therapy; PS, photosensitizer; ROS, reactive oxygen species; DNA, deoxyribonucleic acid; $^1O_2$, singlet oxygen; EA, edge activator; 1H NMR, 1H nuclear magnetic resonance; PDI, polydispersity index; DPBF, 1,3-diphenylisobenzofuran; PBS, phosphate buffered saline; MB, methylene blue; DMSO, dimethyl sulfoxide; SP 20, Span 20; TW 80, Tween 80; MC, methylene chloride; DMEM, Dulbecco's modified Eagle medium; MPa, methyl pheophorbide-a; DW, distilled water; FBS, fetal bovine serum; RSD, relative standard deviation; EE, entrapment efficiency; LA, loading amount; NC, negative control; OD, optical density; PC, positive control; SD, standard deviation; IC50, inhibitory medium concentration values.

■ REFERENCES

(1) Kim, B. Y.; Rutka, J. T.; Chan, W. C. Nanomedicine. *N. Engl. J. Med.* **2010**, *363*, 2434−2443.

(2) Stratton, M. R.; Campbell, P. J.; Futreal, P. A. The cancer genome. *Nature* **2009**, *458*, 719−724.

(3) Gu, W.; Meng, F.; Haag, R.; Zhong, Z. Actively targeted nanomedicines for precision cancer therapy: Concept, construction, challenges and clinical translation. *J. Control. Release.* **2021**, *329*, 676−695.

(4) Mahadik, N.; Bhattacharya, D.; Padmanabhan, A.; Sakhare, K.; Narayan, K. P.; Banerjee, R. Targeting steroid hormone receptors for anti-cancer therapy—A review on small molecules and nanotherapeutic approaches. *Wiley Interdiscip. Rev.: Nanomed. Nanobiotechnol.* **2022**, *14*, No. e1755.

(5) (a) Kolishetti, N.; Dhar, S.; Valencia, P. M.; Lin, L. Q.; Karnik, R.; Lippard, S. J.; Langer, R.; Farokhzad, O. C. Engineering of self-assembled nanoparticle platform for precisely controlled combination drug therapy. *Proc. Natl. Acad. Sci.* **2010**, *107*, 17939−17944. (b) Hu, C.-M. J.; Zhang, L. Nanoparticle-based combination therapy toward overcoming drug resistance in cancer. *Biochem. Pharmacol.* **2012**, *83*, 1104−1111.

(6) Gabizon, A. A.; Lyass, O.; Berry, G. J.; Wildgust, M. Cardiac safety of pegylated liposomal doxorubicin (Doxil/Caelyx) demonstrated by endomyocardial biopsy in patients with advanced malignancies. *Cancer Invest.* **2004**, *22*, 663−669.

(7) Bladé, J.; Sonneveld, P.; Miguel, J. F. S.; Sutherland, H. J.; Hajek, R.; Nagler, A.; Spencer, A.; Robak, T.; Lantz, K. C.; Zhuang, S. H.; et al. Efficacy and safety of pegylated liposomal doxorubicin in combination with bortezomib for multiple myeloma: effects of adverse prognostic factors on outcome. *Clin. Lymphoma, Myeloma Leuk.* **2011**, *11*, 44−49.

(8) Meredith, A.-M.; Dass, C. R. Increasing role of the cancer chemotherapeutic doxorubicin in cellular metabolism. *J. Pharm. Pharmacol.* **2016**, *68*, 729−741.

(9) (a) Thotakura, N.; Panjeta, A.; Negi, P.; Preet, S.; Raza, K. Doxorubicin-Loaded Mixed Micelles for the Effective Management of Skin Carcinoma: In Vivo Anti-Tumor Activity and Biodistribution Studies. *AAPS PharmSciTech* **2021**, *22*, 130−212. (b) Pinto, C. M.; Horta, L. S.; Soares, A. P.; Carvalho, B. A.; Ferreira, E.; Lages, E. B.; Ferreira, L. A.; Faraco, A. A.; Santiago, H. C.; Goulart, G. A. Nanoencapsulated Doxorubicin Prevents Mucositis Development in Mice. *Pharmaceutics* **2021**, *13*, 1021. (c) Laxmi, P.; Varma, A.; Pai, A.; Sathyanarayana, M. B. Experimental data of fabricated co-crystals of doxorubicin hcl with flavonoids. *Indian J. Pharm. Educ. Res.* **2019**, *53*, S225−S230.

(10) Dos Santos, A. F.; De Almeida, D. R. Q.; Terra, L. F.; Baptista, M. S.; Labriola, L. Photodynamic therapy in cancer treatment-an update review. *J. Cancer Metastasis Treat.* **2019**, *2019*, 25.

(11) (a) Davila, M. L. Photodynamic therapy. *Gastrointest. Endosc. Clin. North Am.* **2011**, *21*, 67−79. (b) Agostinis, P.; Berg, K.; Cengel, K. A.; Foster, T. H.; Girotti, A. W.; Gollnick, S. O.; Hahn, S. M.; Hamblin, M. R.; Juzeniene, A.; Kessel, D.; et al. Photodynamic therapy of cancer: an update. *Ca-Cancer J. Clin.* **2011**, *61*, 250−281.

(12) Wilson, B. C.; Patterson, M. S. The physics, biophysics and technology of photodynamic therapy. *Phys. Med. Biol.* **2008**, *53*, R61−R109.

(13) Huang, Y. Y.; Balasubramanian, T.; Yang, E.; Luo, D.; Diers, J. R.; Bocian, D. F.; Lindsey, J. S.; Holten, D.; Hamblin, M. R. Stable synthetic bacteriochlorins for photodynamic therapy: role of dicyano peripheral groups, central metal substitution (2H, Zn, Pd), and Cremophor EL delivery. *ChemMedChem* **2012**, *7*, 2155−2167.

(14) Lee, S.-J. H.; Jagerovic, N.; Smith, K. M. Use of the chlorophyll derivative, purpurin-18, for syntheses of sensitizers for use in photodynamic therapy. *J. Chem. Soc., Perkin trans.* **1993**, *19*, 2369−2377.

(15) (a) Kim, J.-E.; Yoon, I.-S.; Cho, H.-J.; Kim, D.-H.; Choi, Y.-H.; Kim, D.-D. Emulsion-based colloidal nanosystems for oral delivery of doxorubicin: improved intestinal paracellular absorption and alleviated cardiotoxicity. *Int. J. Pharm.* **2014**, *464*, 117−126. (b) Ravindranath, V.;

Chandrasekhara, N. Absorption and tissue distribution of curcumin in rats. *Toxicology* **1980**, *16*, 259−265.
(16) Hasibi, F.; Nasirpour, A.; Varshosaz, J.; García-Manrique, P.; Blanco-López, M. C.; Gutiérrez, G.; Matos, M. Formulation and characterization of Taxifolin-loaded lipid nanovesicles (Liposomes, Niosomes, and Transfersomes) for beverage fortification. *Eur. J. Lipid Sci. Technol.* **2020**, *122*, 1900105.
(17) Chaudhary, H.; Kohli, K.; Kumar, V. Nano-transfersomes as a novel carrier for transdermal delivery. *Int. J. Pharm.* **2013**, *454*, 367−380.
(18) Opatha, S. A. T.; Titapiwatanakun, V.; Chutoprapat, R. Transfersomes: A promising nanoencapsulation technique for transdermal drug delivery. *Pharmaceutics* **2020**, *12*, 855.
(19) El Maghraby, G.; Williams, A. C.; Barry, B. Interactions of surfactants (edge activators) and skin penetration enhancers with liposomes. *Int. J. Pharm.* **2004**, *276*, 143−161.
(20) El Zaafarany, G. M.; Awad, G. A.; Holayel, S. M.; Mortada, N. D. Role of edge activators and surface charge in developing ultradeformable vesicles with enhanced skin delivery. *Int. J. Pharm.* **2010**, *397*, 164−172.
(21) Kashyap, D.; Tuli, H. S.; Yerer, M. B.; Sharma, A.; Sak, K.; Srivastava, S.; Pandey, A.; Garg, V. K.; Sethi, G.; Bishayee, A. Natural product-based nanoformulations for cancer therapy: Opportunities and challenges. *Semin. Cancer Biol.* **2021**, *69*, 5−23.
(22) (a) Nguyen, P. V.; Hervé-Aubert, K.; Chourpa, I.; Allard-Vannier, E. Active targeting strategy in nanomedicines using anti-EGFR ligands−A promising approach for cancer therapy and diagnosis. *Int. J. Pharm.* **2021**, *609*, 121134. (b) Alavi, M.; Hamidi, M. Passive and active targeting in cancer therapy by liposomes and lipid nanoparticles. *Drug Metab. Pers. Ther.* **2019**, *34*(). DOI: 10.1515/dmpt-2018-0032,
(23) (a) Brannon-Peppas, L.; Blanchette, J. O. Nanoparticle and targeted systems for cancer therapy. *Adv. Drug Deliv. Rev.* **2004**, *56*, 1649−1659. (b) Allen, T. M.; Cullis, P. R. Drug delivery systems: entering the mainstream. *Science* **2004**, *303*, 1818−1822.
(24) (a) Zacharis, C. K.; Vastardi, E. Application of analytical quality by design principles for the determination of alkyl p-toluenesulfonates impurities in aprepitant by HPLC. Validation using total-error concept. *J. Pharm. Biomed. Anal.* **2018**, *150*, 152−161. (b) Hassanpour, P.; Hamishehkar, H.; Baradaran, B.; Mohammadi, M.; Shomali, N.; Spotin, A.; Hazratian, T.; Nami, S. An appraisal of antifungal impacts of nanoliposome containing voriconazole on voriconazole-resistant Aspergillus flavus isolates as a groundbreaking drug delivery system. *J. Nanomed. Res.* **2020**, *5*, 90−100.
(25) (a) Ryu, S.; Jin, M.; Lee, H.-K.; Wang, M.-H.; Baek, J.-S.; Cho, C.-W. Effects of lipid nanoparticles on physicochemical properties, cellular uptake, and lymphatic uptake of 6-methoxflavone. *J. Pharm. Investig.* **2022**, *52*, 233−241. (b) Oshiro-Junior, J. A.; Sato, M. R.; Boni, F. I.; Santos, K. L. M.; de Oliveira, K. T.; de Freitas, L. M.; Fontana, C. R.; Nicholas, D.; McHale, A.; Callan, J. F.; et al. Phthalocyanine-loaded nanostructured lipid carriers functionalized with folic acid for photodynamic therapy. *Mater. Sci. Eng. C.* **2020**, *108*, 110462.
(26) (a) Gupta, T.; Singh, J.; Kaur, S.; Sandhu, S.; Singh, G.; Kaur, I. P. Enhancing bioavailability and stability of curcumin using solid lipid nanoparticles (CLEN): A covenant for its effectiveness. *Front. Bioeng. Biotechnol.* **2020**, *8*, 879. (b) Radomska-Soukharev, A. Stability of lipid excipients in solid lipid nanoparticles. *Adv. Drug Deliv. Rev.* **2007**, *38*, 411−418.
(27) Shrestha, R.; Anderson, C. M.; Cardenas, A. E.; Elber, R.; Webb, L. J. Direct measurement of the effect of cholesterol and 6-ketocholestanol on the membrane dipole electric field using vibrational stark effect spectroscopy coupled with molecular dynamics simulations. *J. Phys. Chem. B* **2017**, *121*, 3424−3436.
(28) Li, Z.; Huang, J.; Wu, J. pH-Sensitive nanogels for drug delivery in cancer therapy. *Biomater. Sci.* **2021**, *9*, 574−589.
(29) Makwana, V.; Jain, R.; Patel, K.; Nivsarkar, M.; Joshi, A. Solid lipid nanoparticles (SLN) of Efavirenz as lymph targeting drug delivery system: Elucidation of mechanism of uptake using chylomicron flow blocking approach. *Int. J. Pharm.* **2015**, *495*, 439−446.
(30) Zoubari, G.; Staufenbiel, S.; Volz, P.; Alexiev, U.; Bodmeier, R. Effect of drug solubility and lipid carrier on drug release from lipid nanoparticles for dermal delivery. *Eur. J. Pharm. Biopharm.* **2017**, *110*, 39−46.
(31) Haidar, I.; Harding, I. H.; Bowater, I. C.; Eldridge, D. S.; Charman, W. N. The role of lecithin degradation on the pH dependent stability of halofantrine encapsulated fat nano-emulsions. *Int. J. Pharm.* **2017**, *528*, 524−535.
(32) Ahmed, L.; Atif, R.; Eldeen, T. S.; Yahya, I.; Omara, A.; Eltayeb, M. Study the using of nanoparticles as drug delivery system based on mathematical models for controlled release. *Int. J. Eng. Technol.* **2019**, *8*, 52−56.
(33) Ghosal, K.; Chandra, A.; Rajabalaya, R.; Chakraborty, S.; Nanda, A. Mathematical modeling of drug release profiles for modified hydrophobic HPMC based gels. *Die Pharmazie* **2012**, *67*, 147−155.
(34) (a) Kuklenyik, Z.; Jones, J. I.; Gardner, M. S.; Schieltz, D. M.; Parks, B. A.; Toth, C. A.; Rees, J. C.; Andrews, M. L.; Carter, K.; Lehtikoski, A. K.; et al. Core lipid, surface lipid and apolipoprotein composition analysis of lipoprotein particles as a function of particle size in one workflow integrating asymmetric flow field-flow fractionation and liquid chromatography-tandem mass spectrometry. *PloS one* **2018**, *13*, No. e0194797. (b) Dodangeh, M.; Tang, R.-C.; Gharanjig, K. Improving the photostability of curcumin using functional star-shaped polyamidoamine dendrimer: Application on PET. *Mater. Today Commun.* **2019**, *21*, 100620.
(35) (a) Paramasivan, P.; Kumar, J. D.; Baskaran, R.; Weng, C. F.; Padma, V. V. Reversal of doxorubicin resistance in lung cancer cells by neferine is explained by nuclear factor erythroid-derived 2-like 2 mediated lung resistance protein down regulation. *Cancer Drug Resist* **2020**, *3*, 647. (b) Bellance, N.; Furt, F.; Melser, S.; Lalou, C.; Thoraval, D.; Maneta-Peyret, L.; Lacombe, D.; Moreau, P.; Rossignol, R. Doxorubicin inhibits phosphatidylserine decarboxylase and modifies mitochondrial membrane composition in HeLa cells. *Int. J. Mol. Sci.* **2020**, *21*, 1317.
(36) (a) Kim, J.; Jo, Y.-u.; Na, K. Photodynamic therapy with smart nanomedicine. *Arch. Pharm. Res.* **2020**, *43*, 22−31. (b) Bouramtane, S.; Bretin, L.; Pinon, A.; Leger, D.; Liagre, B.; Perez, D. D. S.; Launay, Y.; Brégier, F.; Sol, V.; Chaleix, V. Acetylxylan-pheophorbide-a nanoparticles designed for tumor-targeted photodynamic therapy. *J. Appl. Polym. Sci.* **2021**, *138*, 50799.
(37) Smith, K. M.; Goff, D. A. Synthesis of nickel (II) isobacteriochlorins from nickel (II) complexes of chlorophyll derivatives. *J. Am. Chem. Soc.* **1985**, *107*, 4954−4964.
(38) Alépée, N.; Tornier, C.; Robert, C.; Amsellem, C.; Roux, M.-H.; Doucet, O.; Pachot, J.; Méloni, M.; de Brugerolle de Fraissinette, A. A catch-up validation study on reconstructed human epidermis (SkinEthic™ RHE) for full replacement of the Draize skin irritation test. *Toxicol In Vitro* **2010**, *24*, 257−266.
(39) Chou, T.-C. Drug Combination Studies and Their Synergy Quantification Using the Chou-Talalay Method. *Cancer Res.* **2010**, *70*, 440−446.

https://doi.org/10.1021/acsomega.3c01654
ACS Omega 2023, 8, 16479−16490